Uniaxial nonlinear surface waves

Paul B. Lundquist[1] and David R. Andersen[2]
[1]*Department of Physics and Astronomy, The University of Iowa, Iowa City, Iowa 52242*
[2]*Department of Electrical and Computer Engineering, The University of Iowa, Iowa City, Iowa 52242*
(Received 16 October 1995)

In this paper, we present calculations describing the fundamental and higher-order stationary nonlinear surface waves that exist at the boundary between a nonlinear self-focusing medium and a uniaxial linear medium. Purely TE or TM solutions do not exist. The solutions obtained are elliptically polarized, and the polarization varies as a function of the transverse coordinate normal to the dielectric interface plane. As a result, these nonlinear surface waves exhibit the phenomenon of a self-walkoff in the Poynting vector. Power dispersion curves and simple analytic expressions for the surface wave threshold as a function of the angle between the crystal axis and propagation direction for the surface wave are obtained and presented.

PACS number(s): 42.65.Wi

I. INTRODUCTION

The field of nonlinear integrated optics is rapidly becoming an important one because of its promise in the areas of optical interconnects and optical communications. Nonlinear optical waveguides typically exhibit strikingly different properties than their linear counterparts, including power thresholds in the dispersion relation. Such properties suggest that these nonlinear waveguides may be ideally suited for nonlinear optical signal processing applications.

Many different nonlinear integrated optical waveguides have been proposed and analyzed. In this paper, we wish to focus the reader's attention on the simplest of all possible guiding structures, the single dielectric boundary. Specifically, the questions we address in this paper concern the existence of nonlinear states localized at the boundary. These states are typically named nonlinear surface waves (NSW).

There is a rich literature concerning the NSW, beginning with the original investigation of such waves existing in a structure comprised of a homogeneous linear dielectric bounded by a homogeneous nonlinear self-focusing dielectric [1,2]. These investigations were motivated by experimental evidence suggesting the existence of such a bound state excited by light obliquely incident on the dielectric boundary. Following the initial development various cases have been examined, including multiple dielectric boundaries [3], TE- and TM-type waves [4–9], nonlocal [10] and self-defocusing nonlinearities [11], etc. [12]. However a unifying simplification inherent in all of these investigations has been the assumption that the media exhibit an isotropic dielectric tensor. In this paper, we compute field profiles and dispersion relations for the fundamental and higher-order NSW's that exist in anisotropic dielectric media, specifically at the boundary between a uniaxial linear dielectric and a homogeneous nonlinear self-focusing dielectric. Additionally, we identify the phenomenon of self-walkoff that is characteristic of these waves.

The anisotropic dielectric NSW problem is an important one, motivated by the fact that strain is present to some degree in all coherently grown crystal systems. The strain, whether tensile or compressive, induces an anisotropy in the dielectric tensor through a modification of the crystal band structure near the boundary. Because all nonlinear integrated optical waveguides involve dielectric boundaries, and many proposed waveguide schemes use coherently grown crystals (e.g., nonlinear waveguides fabricated from the GaAs/AlGaAs semiconductor system) it is very important to understand the impact that this underlying anisotropy has on the characteristics of the NSW.

II. PROBLEM FORMULATION

The geometry of the NSW problem we consider here is shown in Fig. 1. A semi-infinite linear uniaxial crystal exists for $z' \geq 0$, and a semi-infinite nonlinear homogeneous crystal exists in the region $z' \leq 0$, where the primed coordinate system represents the crystal axis coordinate system. The uniaxial crystal is characterized by the dielectric tensor:

$$\underline{\epsilon}_{sw} = \begin{bmatrix} \epsilon_z & 0 & 0 \\ 0 & \epsilon_y & 0 \\ 0 & 0 & \epsilon_z \end{bmatrix}. \tag{2.1}$$

For $z' \leq 0$, the nonlinear polarization is described by the relationship

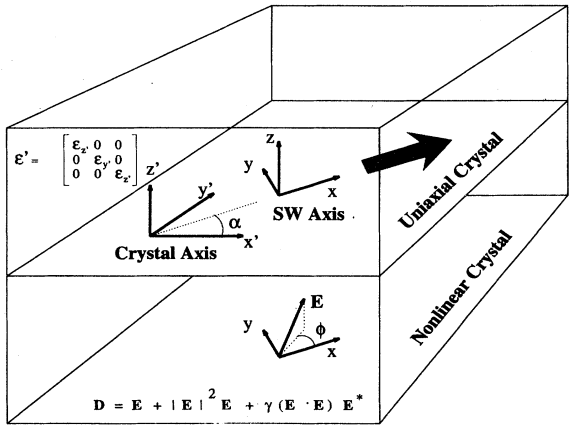

FIG. 1. Uniaxial nonlinear surface wave problem geometry.

$$\mathbf{P}=\left[A|\mathbf{E}|^2\mathbf{E}+\frac{B}{2}(\mathbf{E}\cdot\mathbf{E})\mathbf{E}^*\right], \tag{2.2}$$

where $A=6\chi^{(3)}_{1122}$ and $B=6\chi^{(3)}_{1221}$ are the nonlinear susceptibility parameters, first discussed by Maker and Terhune [13]. For the results presented here, we will consider $A=B$, corresponding to a nonresonant bound electronic nonlinearity, although the technique described in this paper may be applied for arbitrary A and B. The NSW will be described in the unprimed coordinate system, which is rotated through an angle α from the crystal axis. Thus the NSW propagation direction will be along the x axis.

For the problem geometry discussed above, beginning with Maxwell's equations a wave equation can be derived for the NSW field in each of the two dielectrics. The wave equation in the nonlinear medium may be written in normalized form as:

$$\nabla\times(\nabla\times\mathbf{E})=\mathbf{E}+|\mathbf{E}|^2\mathbf{E}+\tfrac{1}{2}(\mathbf{E}\cdot\mathbf{E})\mathbf{E}^* \tag{2.3}$$

and the corresponding wave equation in the linear uniaxial medium is written in normalized form as

$$\nabla\times(\nabla\times\mathbf{E})=\underline{\epsilon}_{sw}\mathbf{E}, \tag{2.4}$$

where

$$\underline{\epsilon}_{sw}=\begin{bmatrix}\epsilon_{xx} & \epsilon_{xy} & 0\\ \epsilon_{xy} & \epsilon_{yy} & 0\\ 0 & 0 & \epsilon_z\end{bmatrix}, \tag{2.5}$$

with

$$\epsilon_{xx}=\epsilon_z\cos^2(\alpha)+\epsilon_y\sin^2(\alpha),$$

$$\epsilon_{yy}=\epsilon_z\sin^2(\alpha)+\epsilon_y\cos^2(\alpha),$$

$$\epsilon_{xy}=\frac{(\epsilon_y-\epsilon_z)}{2}\sin(2\alpha) \tag{2.6}$$

and all dielectric constants have been normalized by the linear dielectric constant in the nonlinear material (i.e., ϵ in the normalized equations may be less than 1).

III. SOLUTION TECHNIQUE

In order to solve the uniaxial NSW problem, we follow the standard technique of computing solutions of the form $\mathbf{E}=\mathscr{E}(z)\exp(inx)$ [where $\mathscr{E}(z)$ is the mode profile for the surface wave] in each of the two media (nonlinear and uniaxial), and then match boundary conditions imposed on the field components at the dielectric interface to obtain a complete solution. In this particular problem, the solution to the wave equation in the linear region can be written analytically as

$$\mathbf{E}=[A_o\mathscr{E}_o e^{n_z^o z}+A_e\mathscr{E}_e e^{n_z^e z}]e^{inx}, \tag{3.1}$$

where the subscripts refer to the ordinary and extraordinary waves, respectively, and the two extinction coefficients are $n_z^o=-(n^2-\epsilon_z)^{1/2}$ for the ordinary wave and $n_z^e=-(n^2\{1+[(\epsilon_y-\epsilon_z)/\epsilon_z]\sin^2(\alpha)\}-\epsilon_y)^{1/2}$ for the extraordinary wave, respectively. The parameter n is the normalized effective refractive index for the surface wave. The vectors $\mathscr{E}^o$ and $\mathscr{E}^e$ are written as

$$\mathscr{E}=\begin{bmatrix}(n^2-\epsilon_z)(n^2-n_z^2-\epsilon_{yy})\\ \epsilon_{xy}(n^2-\epsilon_z)\\ -inn_z(n^2-n_z^2-\epsilon_{yy})\end{bmatrix}, \tag{3.2}$$

where $n_z=n_z^o$ for the ordinary mode, and $n_z=n_z^e$ for the extraordinary mode.

In the nonlinear medium, we can write the mode profile in terms of its three components as

$$\mathscr{E}=\begin{bmatrix}U\\ V\\ iW\end{bmatrix}. \tag{3.3}$$

Because the NSW must remain bound to the interface, the real part of the z component of the Poynting vector must be zero. This constraint forces the z component of $\mathscr{E}$ to be in a phase quadrature with the other two field components, and as a result we obtain from the nonlinear wave equation a set of real equations of motion for the field components U, V, and W:

$$\frac{\partial U}{\partial z}=\frac{1}{n}[-\beta^2W+(1-\gamma)(U^2+V^2)W+(1+\gamma)W^3], \tag{3.4}$$

$$\frac{\partial V}{\partial z}=nQ, \tag{3.5}$$

$$\frac{\partial W}{\partial z}=-\frac{1}{n}\left\{\frac{\frac{2}{n}(1-\gamma)VW\frac{\partial V}{\partial z}+\frac{2}{n}(1-\gamma)UW\frac{\partial U}{\partial z}+U+(1+\gamma)(U^2+V^2)U+(1-\gamma)W^2U}{1+\frac{1}{n^2}[-\beta^2+(1-\gamma)(U^2+V^2)+3(1-\gamma)W^3]}\right\}, \tag{3.6}$$

$$\frac{\partial Q}{\partial z} = -\frac{1}{n}\left[-\beta^2 V + (1+\gamma)(U^2+V^2)V + (1-\gamma)W^2 V\right], \tag{3.7}$$

where $\beta=(n^2-1)^{1/2}$ is the bound mode parameter and Q is defined by Eq. (3.5) so that the system of equations may be written as a coupled set of first order differential equations.

The set of first-order Eqs. (3.4)–(3.7) can then be integrated using standard numerical techniques. The initial condition required for the integration consists of the field amplitude at a distance far from the interface on the nonlinear side. This field amplitude must be sufficiently small so that the nonlinearity is not manifest. In this limit, the initial condition can be characterized by two parameters: ϕ, shown in Fig. 1, which is the polarization angle of the field with respect to the x-y plane, and δ which parametrizes the field amplitude. Using these two parameters, the initial condition is written: $U=\delta\cos(\phi)\exp(\beta z)$, $V=\delta\sin(\phi)\exp(\beta z)$, $W=-n/\beta U$ and $Q=\beta/nV$.

Now that a technique for computing the fields on both sides of the dielectric interface has been established, the appropriate boundary conditions are imposed on the fields at the interface. The tangential boundary condition is written

$$\begin{bmatrix} A_o(z) \\ A_e(z) \end{bmatrix} = \frac{1}{\mathscr{E}^{\,o}_x \mathscr{E}^{\,e}_y - \mathscr{E}^{\,o}_y \mathscr{E}^{\,e}_x} \begin{bmatrix} \mathscr{E}^{\,e}_y & -\mathscr{E}^{\,e}_x \\ -\mathscr{E}^{\,o}_y & \mathscr{E}^{\,o}_x \end{bmatrix} \begin{bmatrix} U(z) \\ V(z) \end{bmatrix}. \tag{3.8}$$

This expression permits an immediate determination of the necessary tangential linear field amplitudes for any interface location z. In an effort to further simplifying the boundary conditions, we make the following observations: B_y will be matched when D_z is matched, and B_z is matched as a result of the assumption that the phase velocity for the entire wave is the same, requiring excitations on both sides of the boundary to propagate as $\exp(inx)$. Thus the problem of matching boundary conditions between the uniaxial linear medium and the nonlinear medium reduces to matching D_z and B_x. The mismatch in these two components can be expressed as:

$$\Delta D_z(z) = iW[1+(U^2+V^2)(1-\gamma)+W^2(1+\gamma)] - \epsilon_z(A_o \mathscr{E}^{\,o}_z + A_e \mathscr{E}^{\,e}_z), \tag{3.9}$$

$$\Delta B_x(z) = nQ - (A_o n^o_z \mathscr{E}^{\,o}_y + A_e n^e_z \mathscr{E}^{\,e}_y). \tag{3.10}$$

Thus the solution technique becomes one of searching the initial condition parameter space to find field distributions for which the mismatches in D_z and B_x are simultaneously zero. Integration of the nonlinear evolution equations in this phase of the work was performed using a seventh-order Adams-Bashforth-Moulton scheme [14], and the initial condition amplitude as well as the grid spacing were varied to assure correct results.

IV. RESULTS

A. Uniaxial NSW modes

A hierarchy of nonlinear uniaxial surface wave solutions was obtained using the technique described above. Each of the solutions was elliptically polarized (purely TE and TM modes are not supported in this problem geometry, for a summary of the argument supporting this conclusion, please see the Appendix) and the polarization varied as a function of the transverse coordinate normal to the interface plane. The solutions obtained are classified according to the number of zero crossings in their various field components (these mode index numbers are similar to those used to classify linear waveguide modes). Interestingly, however, this classification scheme alone is not sufficient to uniquely identify each of the surface wave modes. An alphabetic designator was also used to distinguish qualitatively dissimilar solutions with the same mode index numbers.

We present results for several of the lowest order nonlinear uniaxial surface wave modes in Figs. 2. Figure 2(a) illustrates the field profile and Poynting vector computed for the [001] mode, the lowest-order mode attainable in the uniaxial NSW geometry. The presence of the single zero crossing in the z component of the field for this solution is a result of the differing extinction coefficients for different polarizations in the uniaxial medium. This zero crossing gives rise to a rather unique characteristic of these uniaxial NSW solutions, and that is the existence of a peaked field profile on the linear side of the dielectric boundary. This peak is not found in the homogeneous NSW case and is a consequence of the uniaxial nature of the linear medium.

Figure 2(b) illustrates the field profile and Poynting vector obtained for the [102] mode. In this case, the additional zero crossings are manifest, corresponding to the higher-order mode number. Figures 2(c), 2(d), 2(e), and 2(f) illustrate the field profile and Poynting vector obtained for the [110], [211a], [211b], and [312] modes, respectively. These six modes represent the six lowest-order modes for the uniaxial NSW system.

The [211a] mode and the [211b] mode are interesting to examine. Both of these modes exhibit the same number of zero crossings, however the qualitative nature of the field profiles are quite different. The [211a] field profile closely resembles the [110] field profile with components U and W shifted in phase by 180°. The presence of the two field extinction coefficients in the uniaxial medium modifies the mode index and forces a slight nondegeneracy in the power contained the two modes. A similar effect is present when the [211b] and [312] modes are examined.

B. Poynting vector self-walkoff

In order to examine the polarization characteristics of the uniaxial NSW, we highlight the [211a] mode in Fig. 3. In this figure are plotted the y and z components of the electric field vector (the x component is small enough to be neglected in a plot of this type). As illustrated in the figure, the polarization is essentially elliptical in the y-z plane, with the characteristics of the ellipse changing as a function of position in the transverse direction normal to the interface plane. Such a rotation polarization ellipse gives rise to a Poynting vector that also varies as a function of the transverse position normal to the interface plane. In fact, the largest component of the Poynting vector lies in the x direction, as expected, however each of the intensity lobes of the surface wave have a component of the Poynting vector oriented in the y direction. This y component gives rise to a phenomenon we have called self-walkoff. The energy in the wave at various positions z propagates in slightly different directions. In fact, the

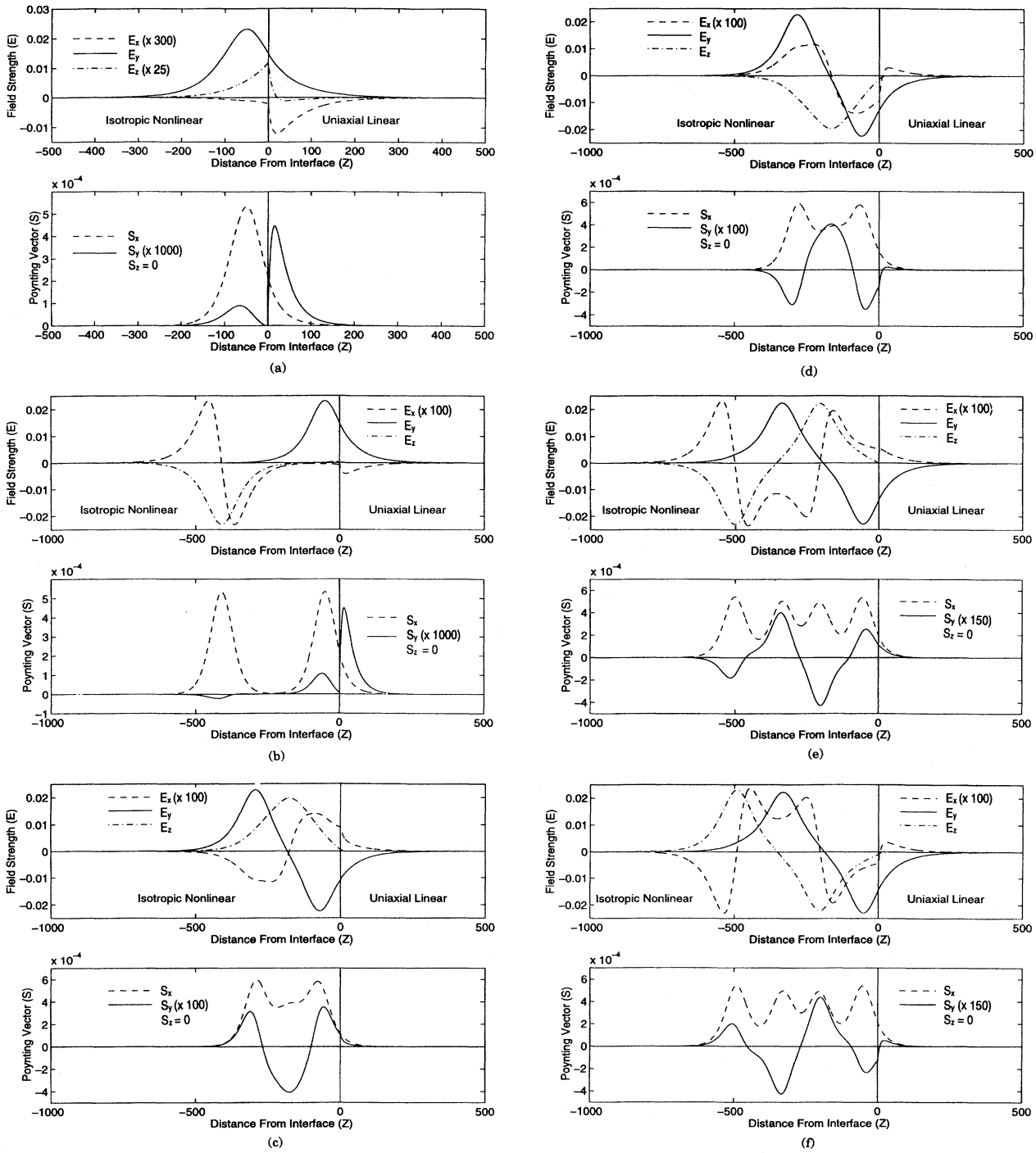

FIG. 2. Electric field and Poynting vector profiles for the six lowest-order uniaxial NSW modes. Parameters used in computing these results are: $\alpha=0.4$, $\epsilon_x=\epsilon_z=0.99\epsilon_{\text{lin}}$, $\epsilon_y=1.002\epsilon_{\text{lin}}$. ϵ_{lin} is the linear dielectric constant in the nonlinear material. The following modes are shown: (a) [001], (b) [102], (c) [110], (d) [211a], (e) [211b], and (f) [312]. All quantities plotted are normalized (unitless).

NSW typically organizes itself so that adjacent intensity lobes possess alternating positive and negative y components of the Poynting vector. This phenomenon is particularly obvious in the [312] mode, and is illustrated in Fig. 4. The alternating nature of this walkoff leads to the term, stratified self-walkoff. Although this does not cause a problem for the existence of the uniaxial wave theoretically, it is unclear what the impact of this self-walkoff will be in an experimental implementation of the uniaxial NSW.

C. Power dispersion curves

The power dispersion curve for the uniaxial NSW is plotted in Fig. 5 for the six different modes illustrated in Fig. 2.

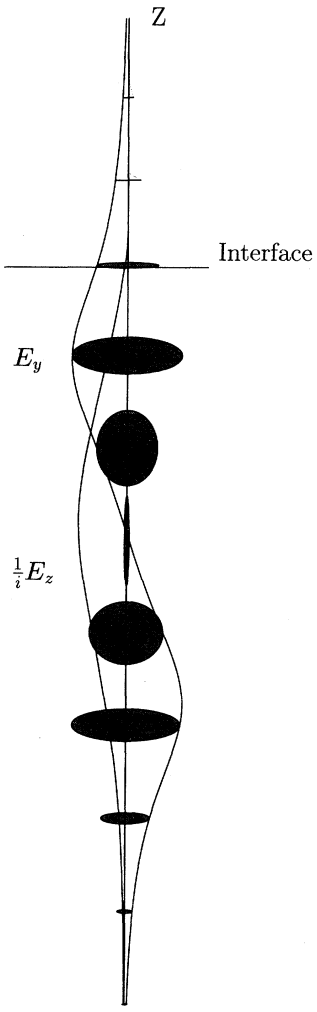

FIG. 3. Illustration of the transverse z dependence of the polarization ellipse of the [211a] mode (the x component of the field is sufficiently small that it may be ignored).

As is typical for the more familiar guided modes (e.g., linear guided modes), as the mode index increases, the power contained in the mode increases. Each of the modes exhibits the characteristic power and mode index thresholds characteristic of NSW's in general. A feature of the uniaxial NSW, however, is that it is possible to adjust these thresholds by angle tuning the crystal relative to the propagation direction (in other words, by varying α) [15]. The relationship between α and the mode parameter cutoff is plotted in Fig. 6. and is given by

$$\beta_c=\left(\frac{\epsilon_y\epsilon_z}{\epsilon_z\cos^2\alpha+\epsilon_y\sin^2\alpha}-1\right)^{1/2}. \tag{4.1}$$

The angle at which the mode parameter cutoff approaches zero is given by

$$\alpha_c=\cos^{-1}\left[\frac{\epsilon_y(1-\epsilon_z)}{\epsilon_y-\epsilon_z}\right]^{1/2}. \tag{4.2}$$

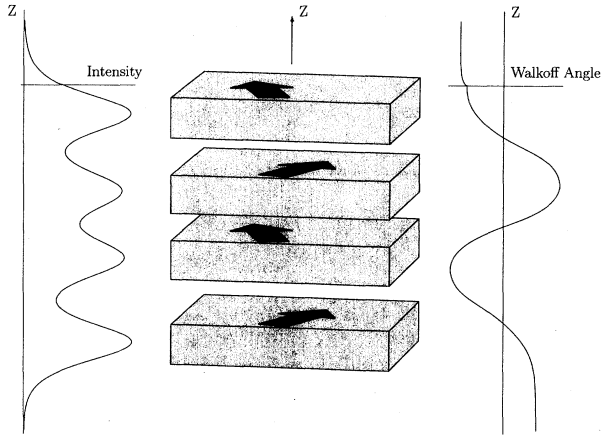

FIG. 4. Schematic illustration of the stratified self-walkoff phenomenon that occurs as a result of the anisotropic character of the linear medium. Each of the intensity lobes of the uniaxial NSW propagates in a slightly different direction (walkoff angle). This figure illustrates the behavior of the [312] mode, although all uniaxial NSW modes exhibit similar behavior.

It is interesting to note that at the angle α_c the resulting solutions do not exhibit a power threshold, but exist even in the linear polarization limit. This angle α_c was shown in [15] to exist nearly in the center of the range of allowed *linear* surface wave angles presented in [16]. It should be noted that the angle α in the current paper equals $\pi/2-\phi$ from Ref. [16]. The ability to angle tune the mode parameter β in this fashion suggests that the uniaxial NSW may be more easily observed, because of the extra degree of freedom such angle tuning provides. However, at this point, we are unable to make any comment regarding the stability of the uniaxial NSW, because the solutions rely on a full vector treatment of the Maxwell's equations. Thus they are not amenable to the scalar perturbation-type stability analysis commonly used on

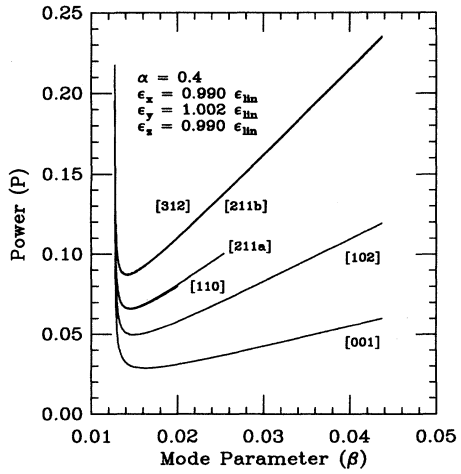

FIG. 5. Nonlinear power dispersion curves for the lowest six uniaxial NSW modes. Parameters used in calculating this result are shown in the figure inset. All quantities plotted are normalized (unitless).

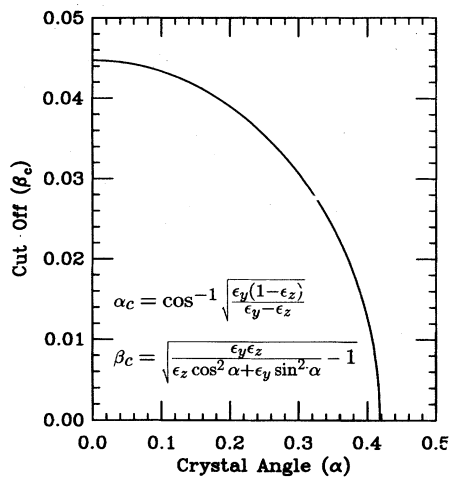

FIG. 6. Mode parameter cutoff (β_c, normalized) as a function of crystal rotation angle (α) in radians for the parameters listed in Fig. 5.

previous NSW problems [17]. Thus stability of these new NSW's remains an open problem.

V. CONCLUSIONS

In this paper we have described our analysis leading to the calculation of uniaxial NSW modes. We have computed the electric field profiles and Poynting vectors for the six lowest-order modes, identified the phenomenon of self-walkoff present in these waves, and computed power dispersion curves and the angle-tuned cutoff in the mode parameter characteristic of these uniaxial NSW's.

ACKNOWLEDGMENT

The authors would like to acknowledge useful discussions with Professor E. G. Gamaly of the Australian National University.

APPENDIX: NONEXISTENCE OF TE AND TM SOLUTIONS

1. TE waves

The fact that TE surface waves can not be supported in a linear uniaxial medium can be explained with a simple geometrical argument. The field on the linear side of the interface must be a linear combination of the two polarization modes $\mathscr{E}^o$ and $\mathscr{E}^e$. To show that a TE mode with polarization

$$\mathbf{F}=\begin{bmatrix}0\\1\\0\end{bmatrix} \tag{A.1}$$

cannot be supported as a surface wave, it is only necessary to show that $\mathbf{F}$ is not in the vector space spanned by $\mathscr{E}^o$ and $\mathscr{E}^e$. This can be expressed as

$$(\mathscr{E}^o\times\mathscr{E}^e)\cdot\mathbf{F}\neq 0, \tag{A.2}$$

and can be proved by contradiction. Assuming the inequality to be an equality one arrives at the expression

$$\mathscr{E}^o_x\mathscr{E}^e_z=\mathscr{E}^e_x\mathscr{E}^o_z. \tag{A.3}$$

Using the explicit solutions for the linear surface modes, Eq. 3.2 can only be satisfied when $\epsilon_y=\epsilon_z$. Therefore it follows that the TE surface waves do not exist in a uniaxial crystal.

2. TM waves

For TM waves, we require $\mathbf{E}_y=0$ and $B_y=0$. At the linear side of the interface, the latter condition can be stated as $\partial/\partial z\mathbf{E}_y=0$. This means that the following two equations must be satisfied:

$$A_o\mathscr{E}^o_y+A_e\mathscr{E}^e_y=0,$$

$$n^o_zA_o\mathscr{E}^o_y+n^e_zA_e\mathscr{E}^e_y=0. \tag{A.4}$$

These are only satisfied when $n^o_z=n^e_z$ which only happens when the linear crystal is isotropic instead of uniaxial. Therefore the TM surface modes are not supported in a uniaxial crystal.

[1] W. J. Tomlinson, Opt. Lett. **5**, 323 (1980).
[2] A. A. Maradudin, Z. Phys. B **41**, 341 (1981).
[3] A. D. Boardman and P. Egan, IEEE J. Quantum Electron. **QE-22**, 319 (1986).
[4] A. D. Boardman, A. A. Maradudin, G. I. Stegeman, T. Twardowski, and E. M. Wright, Phys. Rev. A **35**, 1159 (1987).
[5] D. Mihalache, G. I. Stegeman, C. T. Seaton, E. M. Wright, R. Zanoni, A. D. Boardman, and T. Twardowski, Opt. Lett. **12**, 187 (1987).
[6] S. W. Kang, J. Lightwave Tech. **13**, 391 (1995).
[7] J. Jasinski and K. Gniadek, Opt. Quantum Electron. **26**, 865 (1994).
[8] H. Hayata, M. Nagai, and M. Koshiba, Electron. Lett. **23**, 1305 (1987).
[9] A. D. Boardman and T. Twardowski, Phys. Rev. A **39**, 2481 (1989).
[10] A. B. Aceves, P. Varatharajah, A. C. Newell, E. M. Wright, G. I. Stegeman, D. R. Heatley, J. V. Moloney, and H. Adachihara, J. Opt. Soc. Am. B **7**, 963 (1990).
[11] S. R. Skinner and D. R. Andersen, J. Opt. Soc. Am. B **8**, 759

(1991); D. R. Andersen and S. R. Skinner, *ibid.* **8**, 2265 (1991).
[12] See, e.g., *Nonlinear Surface Electromagnetic Phenomena*, edited by H.-E. Ponath and G. I. Stegeman (North-Holland, Amsterdam, 1991), and references therein.
[13] P. D. Maker and R. W. Terhune, Phys. Rev. **137**, A801 (1965).
[14] L. F. Shampine and M. K. Gordon, *Computer Solution of Ordinary Differential Equations* (Freeman, San Francisco, 1975).
[15] L. Torner, J. P. Torres, F. Lederer, D. Mihalache, D. M. Baboiu, and M. Ciumac, Electron. Lett. **29**, 1186 (1993); J. P. Torres, L.Torner, F. Lederer, D. Mihalache, D. M. Baboiu, and M. Ciumac, J. Opt. Soc. Am. B **11**, 983 (1994).
[16] M. I. D'yakonov, Zh. Eksp. Teor. Fiz. **94**, 119 (1988) [Sov. Phys. JETP **67**, 714 (1988)].
[17] N. V. Vysotina, N. N. Rozanov, and V. A. Smirnov, Zh. Tekh. Fiz. **57**, 173 (1987) [Sov. Phys. Tech. Phys. **32**, 104 (1987)].

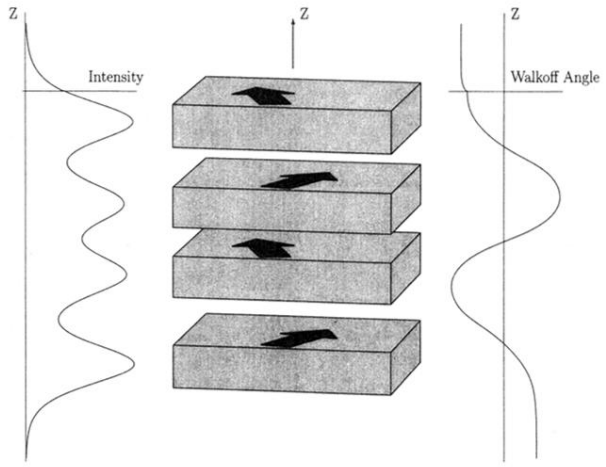

FIG. 4. Schematic illustration of the stratified self-walkoff phenomenon that occurs as a result of the anisotropic character of the linear medium. Each of the intensity lobes of the uniaxial NSW propagates in a slightly different direction (walkoff angle). This figure illustrates the behavior of the [312] mode, although all uniaxial NSW modes exhibit similar behavior.